

Relations between v_z and B_x components in solar wind and their effect on substorm onset

Marina Kubyshkina¹, Vladimir Semenov¹, Nikolai Erkaev^{2,5}, Evgeny Gordeev¹, Stepan Dubyagin³, Natalia Ganushkina^{3,4}, and Maria Shukhtina¹

¹Saint Petersburg State University, Saint Petersburg, Russia.

²Institute of Computational Modelling, Federal Research Center 'Krasnoyarsk Science Center SB RAS', Russia

³Finnish Meteorological Institute, Helsinki, Finland.

⁴University of Michigan, Ann Arbor, MI, USA.

⁵Siberian Federal University, 660041 Krasnoyarsk, Russia.

Key Points:

- Using two substorm onset lists, we show that for 2/3 of all substorm onsets, the $(B_x \cdot v_z)$ product in the solar wind has the same sign as the IMF B_z -component.
- When the signs of the product $(B_x \cdot v_z)$ and the IMF B_z coincide, the asymmetry (bending) of the magnetotail current sheet increases.
- The $(B_x \cdot v_z)$ product in the solar wind during 2/3 of all the time has the sign of IMF B_z , which is a feature of Alfvénic waves propagating from the Sun.

Corresponding author: Marina Kubyshkina, m.kubyshkina@spbu.ru

Abstract

We analyze two substorm onset lists, produced by different methods, and show that the $(B_x \cdot v_z)$ product of the solar wind (SW) velocity and interplanetary magnetic field (IMF) components for 2/3 of all substorm onsets has the same sign as IMF B_z . The explanation we suggest is the efficient displacement of the magnetospheric plasma sheet due to IMF B_x and SW flow v_z , which both force the plasma sheet moving in one direction if the sign of $(B_x \cdot v_z)$ correlates with the sign B_z . The displacement of the current sheet, in its turn, increases the asymmetry of the magnetotail, and can alter the threshold of substorm instabilities.

We study the SW and IMF data for the 15-year period (which comprises two substorm lists periods and the whole solar cycle), and reveal the similar asymmetry in the SW, so that the sign of $(B_x \cdot v_z)$ coincides with the sign of IMF B_z during about 2/3 of all the time. This disproportion can be explained if we admit that about 66% of IMF B_z -component are transported to the Earth's orbit by the Alfvén waves with anti-sunward velocities.

1 Introduction

It is commonly accepted now that the existence of a southward component of Interplanetary Magnetic Field (IMF) is the main driver of magnetospheric activity [Fairfield and Cahill, 1966; Rostoker and Falthammar, 1967; Akasofu, 1975], since the southward direction of IMF is favorable for the magnetic reconnection at the magnetopause [Dungey, 1961]. Yet, the questions on when, why and how does the substorm expansion develop are still under discussion. One of the possible reasons for this long-lasting discussion is the great variability of substorms behavior and substorm onset configurations (see, for example, recent paper by Borovsky and Yakimenko [2017] and references therein.)

One of the important problems in this context is the existence of an external driver for substorm triggering. Recent study by Newell *et al.* [2016] demonstrated a clear dependence of substorm probability on the solar wind speed and claimed that the SW speed is the main predictor for substorm occurrence. That study also showed that any change in IMF B_z or SW speed increases the odds of a substorm if compared to no change, and, especially, if it is a drop in SW speed or a northward turn in IMF B_z . Both of these factors

47 slow down the rate of the magnetic field merging on the dayside magnetopause, but they
48 do not significantly change the geometry of the magnetospheric configuration.

49 Our study stays somewhat aside from the mainstream of substorm research, we ex-
50 plore the solar wind flow v_z -component and the IMF B_x -component as the factors which
51 change the rate of the asymmetry of magnetospheric configuration (see, for exapmle, [*Sergeev*
52 *et al.*, 2008; *Hoilijoki et al.*, 2014; *Tsyganenko and Fairfield*, 2004]) and analyze how do
53 they vary when approaching a substorm onset.

54 At present, there exist a few studies [*Panov et al.*, 2012; *Vörös et al.*, 2014; *Kubyshk-*
55 *ina et al.*, 2015; *Semenov et al.*, 2015] which explore the substorm behavior in a situation
56 with changing solar wind flow velocity. They show that fast changes in the solar wind
57 flow v_z -component, especially in a situation with nonzero dipole tilt, may facilitate a sub-
58 storm onset. A reason for that may be an additional curving and displacement of magne-
59 topheric plasma sheet which lowers the substorm instability threshold in an asymmetric
60 bent current sheet [e.g., *Kivelson and Hughes*, 1990].

61 However, the v_z -component of the flow velocity is not the only solar wind parameter
62 which causes plasma sheet motion in the vertical (normal to ecliptic plane) direction. The
63 existence of a nonzero B_x -component of IMF results in a displacement of an X-line for
64 the dayside magnetopause reconnection and in the asymmetric magnetic flux circulation
65 in magnetospheric lobes [*Cowley*, 1981; *Reistad et al.*, 2014; *Gordeev et al.*, 2016]. Mag-
66 netic flux imbalance in the northern and southern lobes leads, in turn, to the plasma sheet
67 displacement from its equilibrium position. Depending on the sign of the B_x , the plasma
68 sheet will move up or down in a similar way as it does due to a nonzero v_z -component of
69 the SW flow.

70 Therefore, in the present paper, we investigate the mutual effect of both the SW flow
71 v_z -component and the IMF B_x -component on substorm probability. Section 2 describes
72 the details of motivation of this study, in Section 3 we study the pre-substorm statistics,
73 in Section 4 we examine the solar wind and IMF data, and, finally, in section 5 we put
74 together the results and discuss them.

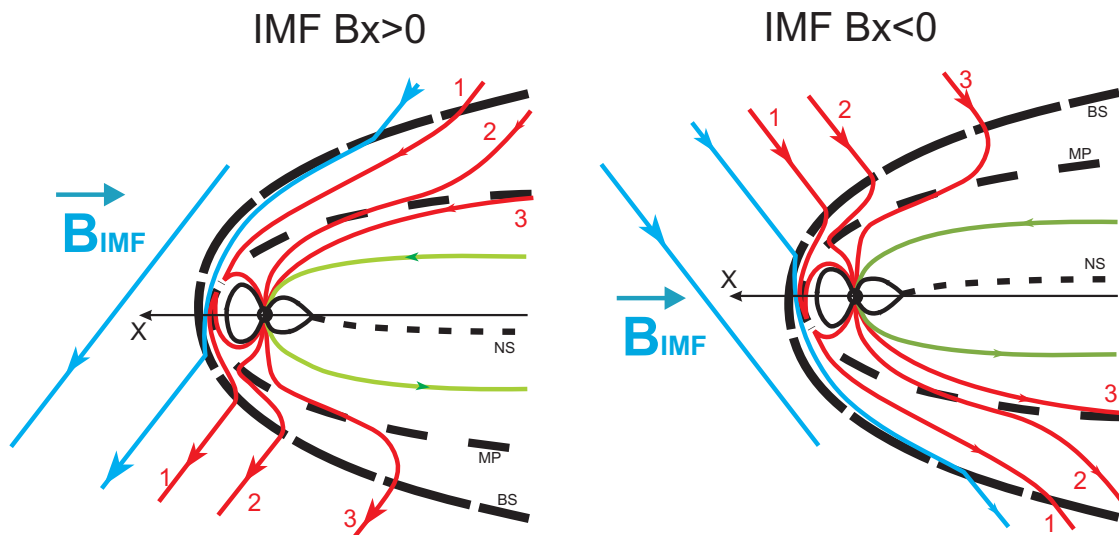
75 **2 Motivation details and background**

76 The existence of the negative IMF B_z (here and below in this section we use Geo-
77 centric Solar Magnetic (GSM) coordinates) is one of the key requirements for a magneto-

78 spheric substorm initiation. Yet, it is also clear that there exist other factors which force
 79 or slow down the substorm onset and vary the amount of energy stored during the growth
 80 phase and released during the expansion phase.

81 If, based on previous works [Kivelson and Hughes, 1990; Panov et al., 2012; Kubyshk-
 82 ina et al., 2015; Semenov et al., 2015], we admit that the increased asymmetry of the mag-
 83 netotail configuration lowers the threshold for substorm triggering instability, we need to
 84 check how do the SW v_z -component and the IMF B_x -component change the position of
 85 the magnetospheric plasma sheet.

86 Following the direction of the solar wind plasma flow, the magnetospheric plasma
 87 sheet will move up from the ecliptic plane under positive solar wind flow velocity compo-
 88 nent v_z and down under negative v_z , irrespective of the sign of the IMF B_z .



89 **Figure 1.** The directions of plasma sheet motion in the presence of positive (left) and negative (right) IMF
 90 B_x component for southward IMF B_z . The blue lines correspond to IMF lines, the red lines are the recon-
 91 nected magnetospheric-IMF lines, the green lines are Earth's magnetotail field lines. The thick black dashed
 92 lines mark the position of Bow Shock (BS), Magnetopause (MP), and Neutral Sheet (NS)

93 The displacement of the plasma sheet under the nonzero IMF B_x is caused by the
 94 non-symmetric dayside reconnection, when the X-line is shifted from the subsolar point.
 95 As a result, the unbalanced reconnected magnetic fluxes in the southern and northern
 96 magnetotail lobes force the plasma sheet moving up or down from the ecliptic plane (see
 97 [Cowley, 1981; Reistad et al., 2014; Gordeev et al., 2016]). The rate of this displacement

will be large only under negative IMF B_z , when the dayside reconnection is active. This phenomenon is illustrated in Figure 1, adopted from Cowley [1981]. Under negative IMF B_z , the plasma sheet will move down with positive B_x -component, and plasma sheet will move up the equatorial plane with the negative B_x -component.

After we compare the plasma sheet reaction to the non-radial SW plasma flow and non-zero IMF B_x , we see that when IMF B_z is negative, the plasma sheet moves up with $B_x < 0$ and with $v_z > 0$, and the plasma sheet goes down with $B_x > 0$ and with $v_z < 0$. Thus, the rate of plasma sheet displacement will be maximal if the sign of a product ($v_z \cdot B_x$) is the same as the sign of the B_z .

If the substorm onset happens under positive IMF B_z , usually it means that the IMF B_z changes its sign from negative to positive in a late growth phase. In this case, when the IMF B_z turns northward, the dayside reconnection stops and the previously (during the period with negative B_z) shifted plasma sheet starts to move in the opposite direction (up for B_x positive and down for B_x negative). Thus, the current sheet displacement due to the existence of the nonzero B_x and v_z will maximize if $(v_z \cdot B_x) > 0$, i.e., again, has the same sign as IMF B_z .

If we assume that the displacement of the plasma sheet is a favorable factor for a substorm onset, we would expect that a number of substorms, which start under the IMF B_z and $(v_z \cdot B_x)$ with the same signs should be larger than the number of substorms which start when the signs of the B_z and $(v_z \cdot B_x)$ are opposite.

3 Data analysis: Substorm Activity

To verify the above suggestion, we used the two principally different substorm databases:

- 1) the list of substorms from Frey *et al.* [2004], which is based on FUV data from IMAGE satellite and contains 4193 substorm onsets during 2000 to 2005;
- 2) the list of substorms from SUPERMAG ground-based magnetic observations (<http://supermag.jhuapl.edu/substorms/>) based on automatic analysis of AL index behavior which contains 18807 substorm onsets during 2000-2010, the period which comprises the period of the Frey *et al.* [2004] data list and also includes both minimum and maximum of the solar cycle activity.

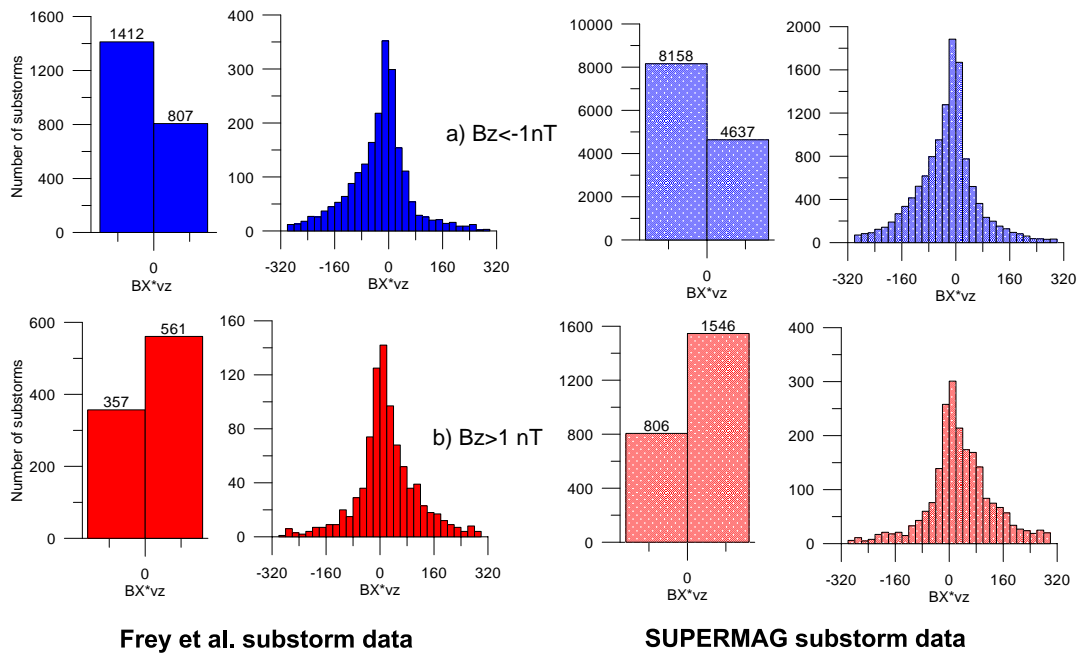
Each database was complemented with OMNI data, containing 5-minute values of IMF and solar wind flow velocity for one hour preceding the substorm onsets. After that, all the substorms were divided into two groups: those which started during southward B_z ($B_z < -1$ nT) and those which began under northward B_z ($B_z > 1$ nT). We used only those onsets, where OMNI data (for both magnetic field and solar flow) was available at the onset time. We excluded the near-zero values of B_z to avoid possible uncertainties, since the sign of B_z is crucial for our analysis. For *Frey et al.* [2004] data the number of exclusions with $-1 < B_z < 1$ was equal to 880 onsets (out of 3989 which had the OMNI data), and for SUPERMAG data set we had 2966 exclusions (out of 18114 onsets with the OMNI data).

The resulting distributions of a number of substorms with different $(v_z \cdot B_x)$ values at the time of a substorm onset (5-min averaged) are given in Figure 2 for both lists of substorms and in two types of histograms: the two-column histogram gives the numbers of substorms with all positive and all negative occurrences of $(v_z \cdot B_x)$, and the 20-column histogram shows a more detailed distribution.

The top row of Figure 2 shows the discussed distributions only for the substorms, which started under negative IMF B_z , with two histograms on the left for *Frey et al.* [2004] substorm list and two histograms on the right for SUPERMAG substorm list. Both substorm lists give the same imbalance in the number of substorms with different signs of $(v_z \cdot B_x)$, the number of substorms which started under negative $(v_z \cdot B_x)$ is almost twice (1.75 times) larger than the number of substorms which started under positive $(v_z \cdot B_x)$ (see two-columns histograms in Figure 2a). Also, it is important to note, that this difference is well reproduced in each pair of bins (positive and negative) of 20-columns histograms, and becomes even larger for the larger values of $(v_z \cdot B_x)$ (see Figure 2a).

The bottom row of Figure 2 gives the same histograms for the substorms with the onsets under positive IMF B_z ($B_z > 1$ nT). The total number of these substorms is much smaller, their intensity is small on average, but the distributions are very similar, with almost twice overage of substorms which started under positive values of $(v_z \cdot B_x)$ (see two-columns histograms in Figure 2b), and with more notable differences in substorm numbers for larger values of $(v_z \cdot B_x)$ (see 20-columns histograms in Figure 2b).

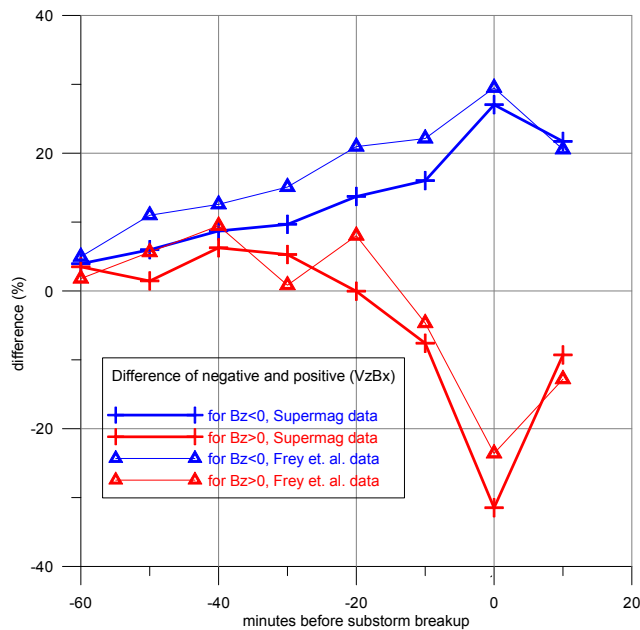
The next important question is if the distribution which we observe near a moment of a substorm onset remains unchanged throughout the growth phase? To check it, we



142 **Figure 2.** Histograms for the number of substorms with different values of $(v_z \cdot B_x)$, measured near the time
 143 of a substorm onset, for two substorm lists (on the right and on the left) and for both signs of IMF B_z (a and b
 144 - top and bottom).

162 made the time series of 12 two-column histograms for both lists of substorms (the same
 163 as those in Figure 2) for twelve 5-min averaged points before the onset (for simplicity we
 164 used the same one-hour period as a growth phase for all the substorms). Using those his-
 165 tograms, we tracked how the relative number of the events for which $(v_z \cdot B_x)$ is posi-
 166 tive/negative changes during the growth phase (or more precisely, during one hour be-
 167 fore the substorm onset). The results are given in Figure 3. Each point on this plot is ob-
 168 tained as a relative difference (in percent) between the number of the events when $(v_z \cdot B_x)$
 169 was negative at a given time before onset, and the number of the events when $(v_z \cdot B_x)$
 170 was positive at the same time (i.e. the difference between 2 bins in the 2-columns his-
 171 tograms), normalized by the total number of substorms under the given sign of IMF B_z .
 172 Blue lines are used for the substorms which start under $(B_z < -1 \text{ nT})$, and red lines - for
 173 the substorms with the onsets under $(B_z > 1 \text{ nT})$, the points from SUPERMAG database
 174 are marked by crosses and the points for *Frey et al.* [2004] substorm database are marked

175 by triangles. Substorm onset is marked by zero on the horizontal axis. We see that the
 176 difference between the number of events where the sign of $(v_z \cdot B_x)$ coincides with the sign
 177 of B_z increases before a substorm onset and maximizes close to an onset (note that we use
 178 5-minute averages for B_x and v_z). From Figure 3 one can also see that for both databases,
 179 the lines look quite similar, they start at less than 5% difference at the beginning of the
 180 growth phase (or, more precisely, one hour before an onset) and reach almost the same
 181 maximal value of about 30%, which means almost twofold difference between the number
 182 of substorms with the same sign of B_z and $(v_z \cdot B_x)$ and the number of substorms with the
 183 opposite signs of those. At the same time, there is a certain distinction in the behavior of
 184 red and blue lines (for positive and negative B_z); while the blue lines show a gradual in-
 185 crease during the whole period of one hour with a more steep rise in last ten minutes, the
 186 red lines remain at approximately the same values during first 30-40 minutes of a growth
 187 phase, and then steeply go down in the last 20 minutes before a substorm onset, change
 188 sign and reach maximum close to an onset.



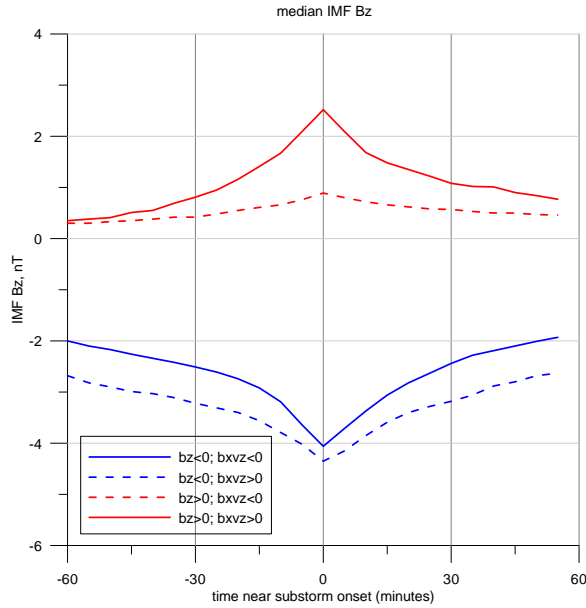
189 **Figure 3.** Time dependence of the difference between the number of the events when $(v_z \cdot B_x)$ was negative
 190 at a given time before onset, and the number of events when $(v_z \cdot B_x)$ was positive at the same time. Blue lines
 191 correspond to the substorm onsets under negative B_z , red lines to those under positive B_z , lines with triangles
 192 show Frey et.al. database, lines with crosses - SUPERMAG database.

193 The above statistics allows one to conclude that 2/3 of magnetospheric substorms
 194 start under the situation when magnetotail plasma sheet moves in the same direction (up
 195 or down the ecliptic plane) due to both IMF B_x and solar wind v_z and since the number
 196 of periods with correlated signs of B_z and $(v_z \cdot B_x)$ increases notably before the substorm
 197 onset, it is reasonable to admit that this signs correlation (which increases the asymmetry
 198 of the magnetotail) can facilitate a substorm onset.

199 Here, it is important to compare our results with a traditional idea of substorm trig-
 200 gering by northward IMF B_z turning [Lyons *et al.*, 1997], which has been strongly criti-
 201 cized in the last ten years (see Morley and Freeman [2007]; Freeman and Morley [2009];
 202 Newell *et al.* [2016]). The results of superposed epoch analysis for the IMF B_z are pre-
 203 sented in Figure 4 separately for all 4 combinations of signs of B_z and $(v_z \cdot B_x)$ at sub-
 204 storm onset. We see that northward IMF B_z turning near onset is observed for both sub-
 205 storm groups with negative IMF B_z . But this turning is much better pronounced in those
 206 substorms which have the same signs of B_z and $(v_z \cdot B_x)$, while the mean values of B_z
 207 amplitudes (and, hence, SW driving) in these substorms are consistently smaller. Thus the
 208 substorm triggering by northward IMF B_z turning is supported by our analysis, and espe-
 209 cially for the cases, when the IMF B_z and $(v_z \cdot B_x)$ have the same signs. On the contrary,
 210 for two groups with positive IMF B_z at onset southward IMF turning is observed, which is
 211 again more pronounced for the substorms with the same sign of B_z and $(v_z \cdot B_x)$.

216 **4 $(v_z \cdot B_x)$ distribution in the Solar Wind**

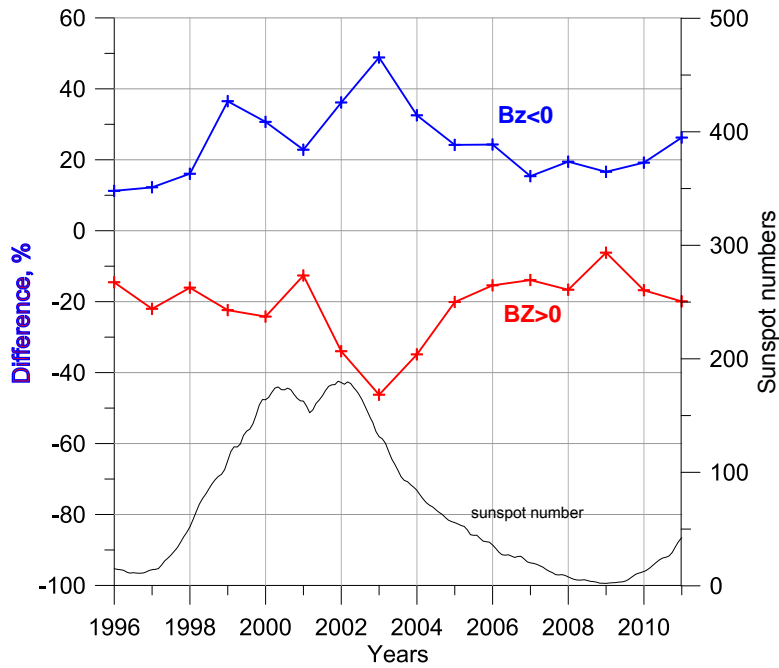
217 After we obtained the above signs correlation of B_z and $(v_z \cdot B_x)$ near a substorm on-
 218 set, it is important to verify if the same correlation is a regular feature in the solar wind.
 219 For consistency, we analyzed the OMNI data for the similar (slightly widened) period,
 220 i.e. for the years 1996-2011. For the solar wind and the IMF components, we used the
 221 Geocentric Solar Ecliptic (GSE) frame, relevant for the solar wind studies. Again, for con-
 222 sistency, we used 5-minutes averages. For each year in this period (1996-2011) we did the
 223 similar (as in Section 3) analysis of distributions of $(v_z \cdot B_x)$ for both positive ($B_z > 1$ nT)
 224 and negative ($B_z < -1$ nT) signs of IMF B_z . For all the 5-minutes periods during the given
 225 year when the IMF B_z was negative (< -1 nT) we calculated the number of 5-minute
 226 periods when $(v_z \cdot B_x)$ was negative and the number of 5-minute periods when it was pos-
 227 itive. The difference between these numbers (in percent) normalized by the whole number
 228 of 5-minute periods when IMF B_z was less than -1 nT, calculated for each year, is plotted



212 **Figure 4.** IMF B_z superposed epoch analysis for 4 different substorm classes, which are defined by the
 213 signs of IMF B_z and $(v_z \cdot B_x)$ near the onset. Blue lines correspond to the ensemble medians for substorms
 214 which started under negative B_z , red lines for those, which started under positive B_z ; solid lines show the
 215 result for same signs of B_z and $(v_z \cdot B_x)$, dashed lines for opposite.

229 in Figure 5 with the blue line. After that, the same procedure was performed for the pe-
 230 riods when the IMF B_z was positive (> 1 nT). The red line in Figure 5 shows the same
 231 relative difference, calculated for the periods, with IMF $B_z > 1$ nT. The Wolf Numbers are
 232 given in black for reference.

236 The resulting Figure 5 demonstrates the same type of imbalance as was obtained in
 237 Section 3. The values from the blue line are always positive; the red line gives only neg-
 238 ative values (i.e., the number of periods with the same signs of the IMF B_z and $(v_z \cdot B_x)$
 239 is always greater than the number of periods with the opposite signs of those). In other
 240 words, the sign of the $(v_z \cdot B_x)$ follows more often the sign of IMF B_z , rather than has the
 241 opposite sign. The degree of this imbalance varies with the solar cycle, it reaches maxi-
 242 mal values (almost 50%, which means 3 times excess) soon after the solar maximum, and
 243 becomes much smaller (about 10-15%) at solar minimum. It is interesting to note that a
 244 very similar behavior of the substorm occurrence rates throughout a solar cycle was re-
 245 ported in *Tanskanen* [2009].



233 **Figure 5.** The normalized annual difference between the number of 5-minute periods with negative and
 234 positive ($v_z \cdot B_x$) (in percent), calculated for the times when IMF B_z was less than -1 nT (blue line) or IMF B_z
 235 was greater than +1 nT (red line). The black line gives the sunspot numbers.

246 5 Discussion and Conclusions

247 Our analysis showed that almost twice larger number of substorms onsets are ob-
 248 served in the periods when the IMF and SW parameters B_z and $(v_z \cdot B_x)$ have the same
 249 signs, if compared to the periods when those signs are opposite. These are the periods
 250 when the magnetotail plasma sheet is forced to move in the same direction (up or down
 251 from the ecliptic plane) due to both, the solar wind flow velocity and the interplanetary
 252 magnetic field B_x -component. We also showed that the difference between the number of
 253 events with positive and negative values of $(v_z \cdot B_x)$ increases during the period of a
 254 growth phase, which may be interpreted as an additional trigger for a substorm onset. In-
 255 deed, if the number of occurrences of $(v_z \cdot B_x)$ with a proper sign (the same as the IMF B_z
 256 has) increases closer to an onset, it means that either v_z or B_x changes sign, which results
 257 in the enhancing of the plasma sheet displacement.

258 The statistical analysis of solar wind v_z and IMF B_x and B_z , provided in this study,
 259 shows that in the solar wind, also, the sign of the $(v_z \cdot B_x)$ follows more often the sign of
 260 IMF B_z , rather than has the opposite one.

261 A simple interpretation of these results implies that the imbalance in the number of
 262 periods with different signs of $(v_z \cdot B_x)$ is produced due to the Alfvén-type disturbances,
 263 propagating from the Sun. The importance and geo-effectiveness of Alfvén waves were
 264 discussed in a great number of papers, see *Belcher and Davis* [1971]; *Snekvik et al.* [2013];
 265 *Zhang et al.* [2014], and references therein. Indeed if we assume that the undisturbed solar
 266 wind flows radially with V_{0x} velocity in the Sun-Earth direction (i.e. along the X_{GSE} -axis)
 267 and that the IMF background component is also radial and equals to B_{0x} , then, for a plane
 268 Alfvén-type wave disturbances (\mathbf{b} and \mathbf{v}) propagating along the Sun-Earth line (along the
 269 X_{GSE} axis):

$$270 \quad \mathbf{b} = \mathbf{b}(x + ut) \quad \text{and} \quad \mathbf{v} = \mathbf{v}(x + ut) . \quad (1)$$

271 Here u is the wave velocity in a fixed frame of reference related to Earth, so that

$$272 \quad u = \pm v_A + |V_{0x}|, \quad (2)$$

273 where v_A is the Alfvén velocity, and signs '+' and '-' correspond to anti-sunward and
 274 sunward directions, respectively. The linearized equation of motion then will look like (for
 275 Alfvén-type wave we also put total pressure gradient equal zero: $\nabla P = 0$) :

$$276 \quad \rho \cdot \left(\frac{\partial \mathbf{v}}{\partial t} + V_{0x} \frac{\partial \mathbf{v}}{\partial x} \right) = \frac{1}{4\pi} \cdot (B_{0x} \frac{\partial \mathbf{b}}{\partial x}) . \quad (3)$$

277 where ρ is the plasma mass density. Note, that V_{0x} here is negative, so $V_{0x} = -|V_{0x}|$.

278 Using (2), we substitute (1) to equation (3) and get

$$279 \quad \rho \left(\frac{\partial \mathbf{v}}{\partial x} \right) = \pm \frac{1}{4\pi v_A} \cdot B_{0x} \left(\frac{\partial \mathbf{b}}{\partial x} \right) . \quad (4)$$

280 Equation (4) yields the following relationship between the velocity and magnetic field per-
 281 turbations:

$$282 \quad \rho \cdot \mathbf{v} = \pm \frac{1}{4\pi v_A} \cdot B_{0x} \cdot \mathbf{b} , \quad (5)$$

283 or, for the z-components (and after multiplying by B_{0x}):

$$284 \quad \rho \cdot (v_z \cdot B_{0x}) = \pm \frac{1}{4\pi v_A} \cdot B_{0x}^2 \cdot b_z . \quad (6)$$

285 From the equation (6) one can see that in the case of earthward (anti-sunward) prop-
 286 agating waves the product ($\tilde{v}_z \cdot B_{0x}$) has the same sign as \tilde{b}_z -component.

287 If the Alfvén-type disturbances are born away from the Sun, we expect to observe
 288 two waves: directed to and from the Sun. If the disturbances appear near the Sun, where
 289 the plasma flow velocities are smaller than the Alfvén velocity, we will observe only one
 290 wave, directed earthward. Thus, the excess number of periods with correlated signs of the
 291 IMF B_z and ($v_z \cdot B_x$), reported in Section 4, probably, corresponds to the near-Sun-born
 292 disturbances. Since the more active Sun produces larger amount of Alfvén-type waves, the
 293 portion of ($v_z \cdot B_x$) with the sign of B_z changes from $\sim 3/4$ (difference 50% in Figure 4)
 294 in the years of the solar maximum to $\sim 9/11$ (10% difference in Figure 4) during the solar
 295 minimum.

296 These Alfvén-type disturbances (propagating earthward) more effectively shift and
 297 displace the magnetospheric plasma sheet and break the magnetospheric configuration
 298 symmetry, which, in turn, may facilitate a substorm onset.

299 Based on our findings, we summarize the results in the following items:

- 300 1. The number of substorms, which started when the solar wind and IMF components
 301 product ($v_z \cdot B_x$) had the same sign as the IMF B_z was about twice larger than the
 302 number of substorms with the opposite signs of those at the time of an onset. This
 303 tendency was proved on two substorm onset lists, obtained by different methods.
- 304 2. The analysis of pre-substorm changes in the number of periods with different signs
 305 of ($v_z \cdot B_x$) shows that the number of periods with preferable sign (same as B_z
 306 at breakup) increases progressively during a growth phase and reaches its maxi-
 307 mum in the last 5 minutes near the onset. This effect is especially notable for the
 308 substorms, which start under positive B_z , which means that not only B_z , but also
 309 ($v_z \cdot B_x$) changes its sign before an onset
- 310 3. 11-years statistics shows that similar imbalance exists in the solar wind. The prod-
 311 uct ($v_z \cdot B_x$) has the same sign as B_z during $2/3$ of all the time if we take the whole
 312 solar cycle period. This portion increases to $3/4$ during the years near the solar
 313 maximum, and decreases to $9/11$ in a years near the minimum of solar activity.

314 The last conclusion leads to a suggestion that the ($v_z \cdot B_x$) value may be an important
 315 agent in substorm initiation, forcing an earlier breakup by changing plasma sheet motion

316 direction. This suggestion needs further and more detailed (case) investigations of sub-
317 storm dynamics.

318 **Acknowledgments**

319 We acknowledge the use of NASA/GSFC's Space Physics Data Facility (<http://omniweb.gsfc.nasa.gov>)
320 for OMNI data. For the substorm data we gratefully acknowledge SUPERMAG and Gjer-
321 loev, J. W. (<http://supermag.jhuapl.edu/substorms/>). This work was supported by Russian
322 Foundation for Basic Research grant N 16-05-00470-a and 15-05-00879-a. The research
323 of S. Dubyagin and N. Ganushkina leading to these results was partly funded by the Eu-
324 ropean Union's Horizon 2020 research and innovation programme under grant agreement
325 No 637302 PROGRESS. The work of N. Ganushkina in Michigan was also partly sup-
326 ported by the National Aeronautics and Space Administration under Grant Agreements No.
327 NNX14AF34G and No. NNX17AI48G issued through the ROSES-2013 and ROSE-2016
328 Programmes, respectively. The Authors thank the Academy of Finland for the support of
329 the Space Cooperation in the Science and Technology Commission between Finland and
330 Russia (TT/AVA). We thank V.Sergeev for valuable comments and fruitful discussions.

331 **References**

- 332 Akasofu, S. I. (1975), Roles of north-south component of interplanetary magnetic-field on
333 large-scale auroral dynamics observed by DMSP satellite, *Planet. Space Sci.*, *23*, 1349-
334 1354.
- 335 Belcher, J. W., and L. Davis (1971), Large-amplitude Alfvén waves in the interplanetary
336 medium, *2*, *J. Geophys. Res.*, *76*, 3534-3563.
- 337 Borovsky, J. E., and K. Yakymenko (2017), Substorm occurrence rates, substorm
338 recurrence times, and solar wind structure, *J. Geophys. Res.*, *122*, 2973-2998,
339 doi:10.1002/2016JA023625.
- 340 Cowley S.W.H. (1981), Asymmetry effects associated with the x-component of the IMF in
341 a magnetically open magnetosphere, *Planet. Space Sci.*, *29*, 8, 809-818.
- 342 Dungey, J. W. (1961), Interplanetary magnetic field and the auroral zones. *Phys. Rev. Lett.*,
343 *6*, 47-48.
- 344 Fairfield, D. H., and J. L. J. Cahill (1966), Transition region magnetic field and polar
345 magnetic disturbances, *J. Geophys. Res.*, *71*, 1, 155-169.

- 346 Freeman, M.P., and S.K. Morley (2009), No evidence for externally triggered substorms
 347 based on superposed epoch analysis of IMF Bz. *Geophys. Res. Lett.* 36, L21101.
 348 <http://dx.doi.org/10.1029/2009GL040621>.
- 349 Frey, H. U., S. B. Mende, V. Angelopoulos, and E. F. Donovan (2004), Sub-
 350 storm onset observations by IMAGE-FUV, *J. Geophys. Res.*, 109, A10304,
 351 doi:10.1029/2004JA010607.
- 352 Gordeev, E.I., Sergeev, V.A., Amosova, M.V., Andreeva V.A. (2016), Influence of in-
 353 terplanetary magnetic field radial component on the position of the Earth's magne-
 354 totail neutral sheet, *Geophysical methods of survey the Earth and its subsoil*, 11-21,
 355 doi:10.13140/RG.2.1.4821.6565
- 356 Hoilijoki, S., V. M. Souza, B. M. Walsh, P. Janhunen, and M. Palmroth (2014), Magne-
 357 topause reconnection and energy conversion as influenced by the dipole tilt and the IMF
 358 Bx, *J. Geophys. Res. Space Physics*, 119, doi:10.1002/2013JA019693
- 359 Kivelson, M.G., W.J. Hughes (1990), On The Threshold For Triggering Substorms, *Planet.*
 360 *Space Sci.*, 38, 2, 211-220.
- 361 Kubyshkina, M., N. Tsyganenko, V. Semenov, D. Kubyshkina, N. Partamies and E.
 362 Gordeev (2015), Further evidence for the role of magnetotail current shape in substorm
 363 initiation, *Earth, Planets and Space*, 67, 139, doi:10.1186/s40623-015-0304-1, 2015
- 364 Lyons, L.R., G.T. Blanchard, J.C. Samson, R.P. Lepping, T. Yamamoto, and T. Morreto (1997),
 365 Coordinated observations demonstrating external substorm triggering. *J. Geophys. Res.*,
 366 102, A12, doi:10.1029/97JA02639.
- 367 Morley, S.K., and M.P. Freeman (2007), On the association between northward turnings of
 368 the interplanetary magnetic field and substorm onsets, *Geophys. Res. Lett.*, 34, L08104.
 369 doi:10.1029/2006GL028891.
- 370 P.T. Newell, K. Liou, J.W. Gjerloev, T. Sotirelis, S. Wing, E.J. Mitchell (2016), Substorm prob-
 371 abilities are best predicted from solar wind speed, *Journal of Atmospheric and Solar-*
 372 *Terrestrial Physics*, 146, 28-37, doi:10.1016/J.JASTP.2016.04.019
- 373 Panov, E.V., R. Nakamura, W. Baumjohann, M. Kubyshkina, A. V. Artemyev, V. A.
 374 Sergeev, A. A. Petrukovich, V. Angelopoulos, K.-H. Glassmeier, J. P. McFadden and D.
 375 Larson (2012) Kinetic ballooning/interchange instability in a bent plasma sheet, *J. Geo-*
 376 *phys. Res.*, 117, A06228, doi: 10.1029/2011JA017496.
- 377 Reistad, J. P., N. Østgaard, K. M. Laundal, S. Haaland, P. Tenfjord, K. Snekvik, K. Ok-
 378 savik, and S. E. Milan (2014), Intensity asymmetries in the dusk sector of the pole-

- ward auroral oval due to IMF Bx , *J. Geophys.Res. Space Physics*, *119*, 9497-9507,
doi:10.1002/2014JA020216
- Rostoker, G., and C. G. Falthammar (1967), Relationship between changes in the inter-
planetary magnetic field and variations in the magnetic field at Earth's surface, *J. Geo-
phys. Res.*, *72*, 5853.
- Semenov, V.S., D.I. Kubyshkina, M.V. Kubyshkina, I.V. Kubyshkin, and N. Partamies
(2015), On the correlation between the fast solar wind flow changes and substorm oc-
currence, *Geophysical Research Letters*, *42*, 13, 5117-5124, doi:10.1002/2015GL064806.
- Sergeev, V. A., N. A. Tsyganenko, and V. Angelopoulos (2008), Dynamical response of the
magnetotail to changes of the solar wind direction: an MHD modeling perspective, *Ann.
Geophys.*, *26*, 2395-2402, doi:10.5194/angeo-26-2395-2008.
- Shue, J.-H., P. T. Newell, K. Liou, C. Meng, and S. W. H. Cowley (2002), Interplanetary
magnetic field Bx asymmetry effect on auroral brightness, *J. Geophys. Res.*, *107*, SIA
16-1, doi:10.1029/2001JA000229.
- Snekvik K., E. I. Tanskanen, and E.K.J. Kilpua (2013), An automated identification method
for Alfvénic streams and their geoeffectiveness, *J. Geophys. Res.*, *118*, 5986-5998,
doi:10.1002/jgra.5058.
- Tanskanen E. I. (2009), A comprehensive high-throughput analysis of substorms observed
by IMAGE magnetometer network: Years 1993-2003 examined, *J. Geophys. Res.*, *114*,
doi:10.1029/2008JA013682
- Tsyganenko, N. A., and D. H. Fairfield (2004), Global shape of the magnetotail cur-
rent sheet as derived from Geotail and Polar data, *J. Geophys. Res.*, *109*, A03218,
doi:10.1029/2003JA010062.
- Vörös, Z., G. Fasko, M. Khodanchenko, I. Honkonen, P. Janhunen, and M. Palmroth
312 (2014) Windsack memory COnditioned RAM (CO-RAM) pressure effect: Forced
re- 313 connection in the Earth's magnetotail, *J. Geophys. Res.*, *119*, 6273-6293, 314,
doi:10.1002/2014JA019857
- Zhang, X.-Y., M. B. Moldwin, J. T. Steinberg, and R. M. Skoug (2014), Alfvén waves as
a possible source of long-duration, large-amplitude, and geoeffective southward IMF, *J.
Geophys. Res.*, *119*, 3259-3266, doi:10.1002/2013JA019623.